Convection, cloud-radiative feedbacks and thermodynamic ocean coupling in simple models of the Walker circulation

Adam H. Sobel[1]
Department of Applied Physics and Applied Mathematics
Department of Earth and Environmental Sciences
Columbia University, New York, NY

Christopher S. Bretherton
Department of Atmospheric Sciences
University of Washington, Seattle, WA

Hezi Gildor
Department of Environmental Sciences and Energy Research
Weizmann Institute of Science
Rehovot, Israel

Matthew E. Peters
Department of Atmospheric Sciences
University of Washington, Seattle, WA

submitted to *Ocean-Atmosphere Interaction and Climate Variability*
C. Wang and S.-P. Xie, editors
September 22, 2003

[1]Corresponding author. Full address: Department of Applied Physics and Applied Mathematics, Columbia University, 500 West 120th St., Rm. 217, New York, NY 10027. E-mail: ahs129@columbia.edu

1. Introduction

The tropical climate is controlled by a complex web of feedbacks between diverse physical processes, including moist convection and radiative transfer, large-scale dynamics in both the atmosphere and ocean, and air-sea transfers of energy, moisture, and momentum. To address this complex problem, it seems best to use a broad range of tools, isolating different aspects and operating at different levels of complexity. Simulation at the highest level of realism attainable, using general circulation models (GCMs) is clearly of fundamental importance, but simple models also have a place. Simple models are further from the real system, but closer to the human mind. Understanding means bridging the gap between the real system and the human mind, and simple models provide a necessary part of the bridge.

Here, we describe a set of simple models that focus on aspects of tropical climate dynamics. We focus on feedbacks between deep convection, radiative transfer, the quasi-steady, divergent component of the atmospheric circulation, and the energy budget of the ocean mixed layer. All these processes are represented as simply as possible, so that the feedbacks between them can be interpreted unambiguously. Ocean dynamics and planetary rotation are neglected. In the atmosphere, the variable of greatest importance in the dynamics of these models is moisture.

Our claim is that these models have something useful to teach us about tropical climate dynamics. In many ways the model solutions are inadequate representations of the real system, not only in their level of detail, but even in some important qualitative respects. Nonetheless, we believe

that they have enough in them that is right that they can help us understand the roles of the various physical processes and some important aspects of the feedbacks between them.

2. Underlying model formulation

a. Equations

We use a set of models which differ in detail but share an underlying formulation. Our starting point is the quasi-equilibrium tropical circulation model (QTCM) introduced by Neelin and Zeng (2000) and Zeng et al. (2000). This model represents the vertical structure of the atmospheric circulation by a set of fixed basis functions, two (one barotropic and one baroclinic) for velocity, and one each for temperature and moisture.

If we exclude the barotropic mode, as we will here, the system is essentially of shallow-water type, though coupled to a moisture equation. It thus has much in common with other reduced models of the tropical atmosphere, but is derived from a different set of assumptions, primarily those behind quasi-equilibrium theory for deep convection as embodied by the Betts-Miller scheme Betts (1986) and related theory as reviewed by Emanuel et al. (1994) and Neelin (1997). The reader is referred to Neelin and Zeng (2000) for more on the model formulation. Examples of climate simulations by the full model (nonlinear, two modes for velocity etc.) can be found in subsequent papers by Neelin's group at UCLA (e.g., Zeng et al., 2000; Su and Neelin, 2002).

In addition to the simplifications assumed in deriving the QTCM itself, we make a number of

additional simplifications to obtain the models discussed here:

1. The Weak Temperature Gradient (WTG) approximation(e.g., Sobel and Bretherton, 2000; Sobel et al., 2001; and references therein): we neglect both the tendency and horizontal advection of atmospheric temperature, as both are small terms (compared to diabatic heating and vertical advection of potential temperature) in the tropical free troposphere.

2. As mentioned above, we omit the barotropic mode; the model flow is purely baroclinic.

3. We neglect rotation, and assume slab-symmetry in the meridional direction, leaving horizontal variability only the longitudinal direction (vertical structure is already determined by the QTCM basis functions). These are models only of the purely divergent, or Walker circulation.

4. We simplify the parameterizations of radiation and surface fluxes, as described below.

With all these assumptions, the equations for the atmosphere are:

$$M_s \frac{\partial u}{\partial x} = P - R, \tag{1}$$

$$\hat{b}\frac{\partial q}{\partial t} + A_q u \frac{\partial q}{\partial x} - M_q \frac{\partial u}{\partial x} = E - P. \tag{2}$$

T is the temperature, and q is the specific humidity times the latent heat of vaporization of water (assumed constant) and divided by the heat capacity for air, so that q, like T, has units of degrees.

Both represent deviations from fixed reference profiles, $T_{ref},\ q_{ref}$[1] :

$$\tilde{T}(x,p,t) = T_{ref}(p) + a(p)T(x,t), \tag{3}$$

$$\tilde{q}(x,p,t) = q_{ref}(p) + b(p)q(x,t), \tag{4}$$

where x, p, t are longitudinal distance, pressure, and time, $a(p), b(p)$ are the nondimensional basis functions, and tildes denote the total physical fields. P, R, and E are precipitation, radiative cooling, and evaporation from the sea surface. M_S and M_q are the dry static stability and gross moisture stratification, which in the earlier versions of the QTCM depended on T and q as:

$$M_q = M_{qr} + M_{qp}q, \tag{5}$$

$$M_S = M_{Sr} + M_{Sp}T, \tag{6}$$

with $M_{qr}, M_{qp}, M_{Sr}, M_{Sp}$ constants. In later versions, for reasons to be discussed below (and see Yu et al. 1998), the formula for M_S has been modified to

$$M_S = M_{Sr} + M_{Sp}\max(T,q). \tag{7}$$

The difference $M = M_S - M_q$ is the gross moist stability, an important parameter in analyses of the moist static energy budget (Neelin and Held, 1987; Yu et al., 1998). The order-unity constants

[1]Different profiles were used in different papers reviewed here. Bretherton and Sobel (2002) and Peters and Bretherton (2004) defined T_{ref} and q_{ref} to be solutions in radiative-convective equilibrium, whereas Sobel (2003) and Sobel and Gildor (2004) simply used default profiles from the QTCM. The two choices differ only by constants times $a(p),\ b(p)$, and have no effect on the total solutions.

$\hat{b}$ and A_q are derived from from the Galerkin projection of the original primitive equations on the QTCM basis functions.

The horizontal velocity also has a basis function, $V(p)$, so

$$\tilde{u}(x,p,t) = V(p)u(x,t),$$

which changes sign once with pressure in the troposphere, so that it is positive in the upper troposphere and negative in the lower.

We do not show a momentum equation, because under our assumptions (particularly WTG, no rotation, and slab-symmetry) one is not necessary. The flow is purely divergent, and the divergence $\frac{\partial u}{\partial x}$ is determined by the heating through (1), which states that the heating is balanced by horizontal divergence of dry static energy. u can then be found by integration in x, given boundary conditions. If desired, the momentum equation can be used to infer the pressure perturbations necessary to drive this flow. Hydrostatically, these must be associated with small horizontal temperature perturbations neglected under WTG, e.g., in (1), The validity of WTG can be assessed by checking that these diagnosed temperature perturbations are much smaller than the horizontal. variations of surface temperature.

Although the temperature is assumed horizontally uniform, its value is part of the solution, to satisfy the domain-integrated heat budget:

$$\hat{a}\frac{\partial T}{\partial t} = \frac{1}{L}\int_0^L (P-R)dx, \tag{8}$$

where $x = 0, L$ are the domain boundaries (which may be periodic)[2]

b. Parameterizations

The precipitation, or equivalently convective heating, is parameterized by the simplified Betts-Miller scheme:

$$P = \mathcal{H}(q - T)\frac{q - T}{\tau_c}, \tag{9}$$

where $\mathcal{H}$ is the Heaviside function and τ_c is a specified convective time scale.

Under WTG, $q - T$ can be regarded as the excess of a column-averaged relative humidity r above a convective threshold r_c (at which $q = T$). Bretherton et al. (2004) showed that over the tropical oceans, monthly-mean satellite-observed P is an exponentially increasing function of r. Their results suggest that $\tau_c = 16$ hours was the best match to the above observations. Were one mainly interested in transient variation of convection on daily time scales, rather than (as here) long-term quasi-steady mean behavior, their results would suggest a slightly shorter time scale. Taking this large a value for τ_c allows q to be somewhat larger in heavily precipitating regions than in lightly precipitating regions, introducing complexities due to horizontal moisture advection and, possibly, also due to q-induced horizontal variations of gross moist stability (see section iii.).

A theoretically appealing, though less realistic limit is $\tau_c \to 0$, also known as hard convective adjustment or strict quasi-equilibrium (SQE; Emanuel et al., 1994), in which $q \leq T$ everywhere,

[2]Equation (3) in Sobel (2003) should have been identical to (8) here, but the former erroneously omitted the factor $1/L$ on RHS. The factor L was eventually set to 1, but this had not yet been done at the point where Sobel's (3) was presented.

with the equality holding in convective regions (where $P > 0$). In this case the precipitation is not computed directly. Rather, the divergence can be computed from the moist static energy equation, which is obtained by adding the temperature and moisture equations together, and then the precipitation can be computed from (1), if R is known. The steady-state moist static energy equation is

$$A_q u \frac{\partial q}{\partial x} + M \frac{\partial u}{\partial x} = E - R. \tag{10}$$

Under SQE, in convective regions $q = T$, while T has already been assumed horizontally uniform throughout the domain, so we can drop the horizontal advection term (in convective regions only):

$$M \frac{\partial u}{\partial x} = E - R, \tag{11}$$

which substituted directly in (1) and rearranged yields

$$P = \frac{M_S}{M} E - R(\frac{M_S}{M} - 1). \tag{12}$$

We parameterize evaporation by a bulk formula with fixed surface wind speed and exchange coefficient:

$$E = \frac{q_s^* - b_s q}{\tau_E}, \tag{13}$$

where q_s^* is the saturation specific humidity at the sea surface temperature, b_s is the value of $b(p)$ at the surface pressure, and τ_E is an exchange time scale, kept constant. The neglect of surface wind

speed variations in particular is a strong limitation of these models (which can be relaxed), but is felt to be reasonable at this level of idealization, since the wind speed itself is not modeled particularly well by its quasi-steady divergent component, which is all that these models simulate.

The radiative cooling is parameterized by

$$R = R^{clr} - rP = \frac{T - T_e}{\tau_R} - rP. \tag{14}$$

The first term, R^{clr}, represents clear-sky conditions by relaxation to an equilibrium temperature T_e on a time scale τ_R, while the second models the greenhouse effect of high clouds as proportional to the precipitation with a coefficient r. This cloud-radiative feedback on the atmosphere is assumed to be all in the longwave band. Shortwave variations are assumed to matter only at the surface (i.e. constant shortwave absorption in the atmosphere). The surface forcing, including ocean heat transport and surface longwave radiative energy flux, is modeled by

$$S = S^{clr} - rP, \tag{15}$$

where S^{clr} is the clear-sky value and the term rP models the shortwave cloud-radiative feedback; ocean heat transport and surface longwave are assumed constant. Use of the same coefficient r in (14) and (15) builds in the assumption that longwave and shortwave effects of high clouds cancel at the top of the atmosphere, as is approximately observed (Ramanathan et al., 1989; Harrison et al., 1990; Kiehl, 1994; Hartmann et al., 2001). Since variations in atmospheric shortwave absorption

are neglected, the shortwave modulation represented by (15) only enters the surface energy budget and is therefore irrelevant if a fixed-SST lower boundary condition is used.

c. Lower boundary condition

We use two different lower boundary conditions: fixed SST, and a dynamically passive ocean mixed layer. In the latter case, the thermodynamic equation for mixed layer is

$$C\frac{dT_s}{dt} = S - E, \tag{16}$$

where T_s is the SST and C a bulk heat capacity proportional to the mixed layer depth; C is dimensionless if S and E are expressed in degrees per day and T_s in degrees.

In steady state, (16) tells us that the net surface forcing (ocean heat transport plus surface radiative forcing) must balance evaporation:

$$S = E. \tag{17}$$

Because of the use of the same r in both the longwave and shortwave cloud feedbacks, (11) can be combined with (17), (14), and (15) to yield

$$M\frac{\partial u}{\partial x} = S^{clr} - R^{clr}, \tag{18}$$

which can be combined with (1) to yield, instead of (12),

$$P = \frac{M_S}{M} S^{clr} - (1+r)^{-1}(\frac{M_S}{M} - 1) R^{clr}. \tag{19}$$

In other words, the precipitation is controlled by the *clear-sky* values of the radiative cooling and surface forcing.

3. Specific models and results

a. Specified, time-independent, spatially varying SST; SQE model

The first case we consider is that studied by Bretherton and Sobel (2002), in which the sea surface temperature is specified, time-independent, and has a sinusoidal profile in longitude, with specified amplitude Δ and mean value T_{s0}:

$$T_s = T_{s0} + \Delta \cos(\pi x / L),$$

with T_{s0}, Δ parameters; here the domain extends from $x = -L$ to L. In the convective scheme, SQE is assumed. The aim here is to vary the magnitude of the SST gradient and the value of r, and to see how these modify the extent of the convective region and the strength of the circulation.

For sufficiently small Δ (e.g. 0.1, Fig. 1), convection occurs everywhere, and the equations become linear and analytically tractable. Fig. 1 shows the precipitation and vertical motion for cases with $r = 0$ and $r = 0.2$. Increasing the cloud-radiative feedback increases the precipitation

contrast across the domain and strengthens the circulation.

[Figure 1 about here.]

For Δ larger than about $0.15\ K$, the precipitation becomes zero in part of the domain. This introduces two nonlinearities: that resulting from the nonnegativity of precipitation, and horizontal moisture advection, as the humidity field in the nonprecipitating region is not constrained by SQE (as it is in the precipitating region) so that horizontal gradients develop in response to the SST gradient. Bretherton and Sobel (2002) obtained steady solutions directly, by treating the precipitating and nonprecipitating regions separately and matching them at a boundary which must be determined, together with the tropospheric temperature, as part of the solution.

[Figure 2 about here.]

Fig. 2 shows the solutions for $\Delta SST = 2°$K , again for $r = 0$ and $r = 0.2$. As in the linear case, the cloud-radiative feedback increases the contrast between the regions of low and high SST, now shrinking the precipitating region and intensifying the precipitation and vertical motion there. Solutions with the horizontal moisture advection term omitted are also shown, and we can see that this term also plays an important role in setting the horizontal extent of the precipitating region. Since the low-level flow is convergent into that region, it flows *from* the region of lower humidity, and thus dry air advection suppresses convection near the boundary and pushes the boundary back to higher SST. This effect is not as strong as that of the cloud-radiative feedback for $r = 0.2$.

As r is increased, the convective region shrinks and intensifies further until eventually, for large enough r, no steady solution can be obtained. This indicates the existence of a radiative-convective instability, which can be understood by simple analysis of the eqations. Some manipulation of (1) and (11) using (14) yields:

$$M_{eff}\delta = E - R^{clr}, \tag{20}$$

where we have defined the effective gross moist stability (Su and Neelin, 2002; Bretherton and Sobel, 2002).

$$M_{eff} \equiv \frac{M - rM_q}{1 + r}. \tag{21}$$

As with the definition of the standard gross moist stability, M_{eff} tells us the strength of the mass circulation through a convective region given a rate of moist static energy supply through the vertical boundaries, but where the latter supply comes from the surface fluxes minus total tropospheric radiative cooling in the case of M, now it is defined as the surface fluxes minus only the clear-sky component of the radiative cooling, with the cloud-radiative feedback treated as part of the response. For negative M_{eff}, the system can sustain upward motion ($\delta > 0$) even if the clear-sky component of the radiative cooling removes more moist static energy than the surface fluxes add, because the cloud-radiative feedback more than compensates for the difference. This means that convection can occur spontaneously even where the boundary conditions do not favor it, in the sense that a lack of convection would also be an acceptable steady solution. This is an indication of instability. $M_{eff} = 0$ corresponds to the bifurcation point at which the instability sets in, past which no steady

solution can be obtained.

The very strong response of this model to the cloud-radiative feedback turns out to be misleading in an important way when we consider the coupled atmosphere-ocean system. In the fixed-SST model described above, the cloud-radiative feedback acts as a net energy gain to the system, whose magnitude is determined as part of the solution. Observations show, however, that the net effect of high tropical clouds (the only ones we can presume to model as related directly to precipitation) is approximately zero at the top of the atmosphere (TOA), because the shortwave albedo effect approximately balances the longwave greenhouse effect. Because shortwave absorption in the troposphere is relatively small, the dominant effect of the shortwave albedo of high clouds is to reduce the incident shortwave flux at the surface, cooling the ocean. This important effect is neglected in the fixed-SST model, but is considered below.

As mentioned above, the momentum equation, which is not needed to obtain the solution for the flow, moisture, or precitation fields, can be used to infer the small spatially-varying temperature perturbation which is neglected under WTG. In this model, the amplitude of this perturbation grows as the domain size does, so that WTG is a better approximation for small domains (exactly how small depends on the value of the friction coefficient assumed in the momentum equation). This result is not entirely general, but comes about because of the single vertical mode, and consequent uniformity of friction with height. Shaevitz and Sobel (2004) studied a two-column, nonrotating model of the Walker circulation, with a WTG free troposphere coupled to a boundary layer in which

temperature gradients were *not* neglected, corresponding to an assumed friction which is significant only in the boundary layer. Under this configuration, WTG holds better for larger spatial domains than for smaller ones.

b. Model with a dynamically passive ocean mixed layer

i. Results Sobel (2003) and Peters and Bretherton (2004) considered the system including an ocean mixed layer as represented by (16). The model is then forced not by a given SST distribution, but instead by a given x-dependent surface forcing, $S(x)$. Other differences with the study of Bretherton and Sobel (2002) include generalization from SQE to a finite τ_c, and a linear, rather than sinusoidal forcing [3]:

$$S = S_0 + \Delta S x. \tag{22}$$

For sufficiently small forcing gradient, this system also has a linear regime in which precipitation occurs throughout the entire domain. We focus here on the nonlinear regime, in which both Sobel (2003) and Peters and Bretherton (2004) obtained solutions by numerical integration of the time-dependent equations, as opposed to the steady algorithm used by Bretherton and Sobel (2002).

[Figure 3 about here.]

Fig. 3, taken from Sobel (2003), shows steady solutions for SST, humidity, evaporation, precipitation, and radiative cooling, obtained for $r = 0.2$, $\tau_c = 0.2\ d$, $S_0 = 130\ W\ m^{-2}$, and

[3]Sobel (2003) used the domain $x = [0, 1]$, so that $S = S_0$ at $x = 0$, while Peters and Bretherton (2004) defined the domain symmetrically, so that the domain average of S is equal to S_0.

$\Delta S = 100\ W\ m^{-2}$. We see a qualitatively similar structure in q as in the fixed-SST model, with a relatively large gradient in the nonprecipitating region and a much smaller gradient in the precipitating region, but the gradient is not quite zero in the latter due to the finiteness of τ_c, which allows q to differ slightly from T, and to track the SST to some extent. The SST is strongly controlled by the shortwave cloud feedback. As the surface forcing creates stronger precipitation at larger x, the shortwave albedo effect intensifies and prevents the SST from warming in response to the surface forcing increase. This negative feedback, a local version of the "thermostat" (Ramanathan et al., 1989; Waliser, 1996), turns the precipitating region into a "warm pool" of nearly homogenized SST.

ii. Analytic solution for SQE limit Peters and Bretherton (2004) obtained analytical solutions for the coupled model, in the limit $\tau_c \to 0$ (SQE), and with a linearization of the Clausius-Clapeyron equation so that

$$q_s(T) = q_s(T_{s0}) + \gamma T',$$

with T_{s0} the SST in RCE and T' the departure from T_0. With these assumptions, the atmospheric temperature is equal to the value it would have at radiative-convective equilibrium, with the surface forcing, S, set to its mean value (S_0, in Peters and Bretherton's notation; again in Sobel's notation S_0 is the minimum value of the forcing) over the domain. The horizontal distribution of P is obtained from (19), by noting that R^{clr} is uniform and equal to R_0^{clr}. By also invoking domain-integrated

energy balance, we deduce that the fraction of the domain in which $P > 0$ is

$$f_c = \max(2\frac{R_0^{clr} M_0}{\Delta S M_{s0}}, 1),$$

where ΔS is the variation in S across the domain. In SQE, $q = T$ in the convecting region, so that M_q and thus M are determined once T is. The subscript "0" refers to the RCE value. The warm pool SST is

$$T_s = \frac{\Delta S \tau_E}{\gamma} \frac{M_{eff}}{M_0} x,$$

while the cold pool SST is

$$T_s = \frac{\tau_E}{\gamma}[rE_0 + \Delta S x + \frac{b_s}{\tau_E} \frac{M_0}{M_{qp}}(1 - x/A_c)],$$

where A_c is the size of the convective region, M_{qp} is the proportionality constant relating M_q to q, and b_s is the surface value of $b(p)$. The precipitation is

$$P = P_0 + \frac{\Delta S(x)}{1 + r} \frac{M_{s0}}{M_0} \tag{23}$$

An interesting feature of this solution is that the convective area fraction f_c is independent of the cloud-radiative feedback parameter r, in stark distinction to the fixed-SST case. This is because the precipitation is now controlled by the clear-sky surface forcing, as expressed by (19). Numerical results (not shown) show that even when r is made large enough that large oscillations occur in the convective region (see below), the spatial structure of the *time-mean* precipitation field, including

the value of f_c, changes extremely little from the steady-state values, as long as the simulation is carried out long enough for the statistics to become stationary. Cloud-radiation feedback flattens the SST gradient in the convective region instead of reducing the spatial extent of the convective region.

iii. Dependence on r and τ_c The precipitation, quite unlike the fixed-SST case, is actually slightly weakened by the cloud radiative feedbacks, as can be seen clearly in the analytical expression (23) obtained in the SQE limit. The cloud-radiative feedbacks act to reduce S (which in steady state is equal to E) in convective regions at the same time that they decrease R by the same amount, so that the net forcing of the divergent circulation $E - R$ [see (11)] and therefore the circulation strength is unchanged. In steady state $E = S$, and then using (14) and (15) we have

$$E - R = S^{clr} - R^{clr}.$$

However, the decrease in E results in a decrease in precipitation, since the precipitation must equal evaporation plus moisture convergence, and moisture convergence is the product of the circulation strength and the gross moisture stratification M_q. M_q is a function of q only, and hence is fixed in convective regions in the SQE limit since then $q = T$. The precipitation itself can also be found explicitly in terms of the clear-sky forcings, e.g. by first obtaining (24) below, and then substituting $E = S = S_0 - rP$.

Much of the discussion in this paper, including the analysis immediately above, concerns the

SQE limit $\tau_c \rightarrow 0$. As previously noted, observations have shown suitable values of τ_c to be approximately 16 hours. This is smaller than any other time scale in the problem, but not by so much that deviations from SQE can be assumed unimportant *a priori*. It is reasonable to ask how the solutions may change as τ_c is increased towards realistic values.

As τ_c is increased, q becomes increasingly horizontally non-uniform, in proportion to $\tau_c P$, in the convecting region. Whether these variations in q have other major effects on the simulation depends on how the gross moist stability depends on q. If the formulation (6) is used for M_S, then increases in q, by increasing M_q while M_S does not change, will lead to decreases in M. Consideration of eq. (11) shows that this will lead to increases in upward motion, and hence precipitation, in the convective region. If τ_c is made large enough, M can actually become negative, leading to a strong instability which will cause the solution to blow up.

However, we now believe that this behavior may be unrealistic. Yu et al. (1998) showed that increasing low-level moisture (here q) need not always decrease M. Yu et al. argued that there is another effect, due to variations in the height attained by convection. The higher the convective updrafts go, the larger M_S should become, since air then outflows with higher values of moist static energy. Yu et al. related the height of convection to the degree of instability in the column, which is mostly dependent on near-surface moisture. These considerations have led to the formulation (7). With this formulation [which was not used by Sobel (2003); it was not needed since he used the small value $\tau_c = 0.2\ d$], M becomes nearly independent of τ_c in the convective region, and as a

result the precipitation and other variables exhibit only very small changes as τ_c is increased up to values on the order of 1 d; the changes are sufficiently small that they are not shown in Fig. 3. Thus, in this regime SQE is a good approximation for the purposes of understanding many properties of the steady solutions. On the other hand, when we consider the stability of those solutions to time-dependent perturbations, the picture changes considerably and the model behavior becomes, even within this range $\tau_c \leq 1$ d, quite sensitive to variations in τ_c, as will be discussed in section v. .

iv. Coexistence of evaporation minimum and precipitation maximum In presenting the results from this model, Sobel (2003) emphasized the coexistence of a local minimum in evaporation and maximum in precipitation at $x = 1$. Such a feature is observed, broadly speaking, in the western Pacific warm pool, where light winds render climatological evaporation small although precipitation is large. From the point of view of the moisture budget, this feature is easily explained, as horizontal moisture convergence is the dominant term balancing precipitation and can easily compensate for small evaporation. From the point of view of the moist static energy budget, the situation is not so simple, and the coexistent evaporation minimum and precipitation maximum require some explanation. If radiative cooling and M were both constant, (12) tells us that features in P would have to mimic those in E, albeit with larger amplitude. Leaving aside the possibility of significant variations in M for the moment, we consider the effect of variations in R which do occur. We expect the high clouds associated with the precipitation maximum to reduce radiative cooling. If large enough,

this effect could could cause $E - R$ to have a maximum where E has a minimum, thus making the P maximum consistent with the moist static energy budget there. However, if we parameterize R as a decreasing function of P, as in (14), and neglect horizontal moisture advection (consistent with the SQE limit $\tau_c \to 0$) we do have a problem, as then the only external forcing for the system is again E, and we can rewrite (12) as

$$P = \frac{\frac{M_S}{M_{eff}}(E - R^{clr}) + R^{clr}}{1 + r}. \tag{24}$$

As long as $M_{eff} > 0$, (24) means that if $M_{eff} > 0$ in a region where $P > 0$, gradients in P and E will have the same sign, $\partial P/\partial E > 0$, so one cannot have a minimum where the other has a maximum.

The coexistent evaporation minimum and precipitation maximum therefore require $M_{eff} < 0$. We found in the fixed-SST model that this led to inability to find a solution (strictly, a steady solution, but in fact not even a well-behaved time-dependent solution is obtainable in this case). Strictly, the reason this was true was not that SST was fixed, but that the fixed-SST model assumed SQE. If instead τ_c is finite, the stability criterion for the system is changed, as discussed in more detail in section c. and in Sobel and Gildor (2003). The system is stabilized, and stable steady solutions can be obtained for M_{eff} slightly negative. Horizontal moisture advection in general becomes nonzero for finite τ_c, because q is no longer required to equal T in convective regions and thus may develop horizontal gradients. However, the stabilization derived by Sobel and Gildor

(2003) was obtained while still neglecting horizontal advection, and so does not result from that effect; rather it results from a negative feedback between q and E which occurs when q is allowed to vary in convective regions. Including horizontal advection would render (24) not strictly correct, but for small τ_c horizontal advection is too weak to change the conclusion drawn from inspecting (24), namely that negative M_{eff} is required for a stable steady solution with a coexistent evaporation minimum and precipitation maximum.

So far we have shown that the coexistent evaporation minimum and precipitation maximum, in steady state, requires negative M_{eff} and finite τ_c. We have not said anything specifically about the coupled system vs. the fixed-SST system. Obtaining the coexistent evaporation minimum and precipitation maximum in the coupled system, as in fig. 3, is fairly easy, as long as τ_c is finite, r is large enough to render $M_{eff} < 0$, but not too large (in which case the steady solution becomes unstable to time-dependent disturbances, discussed below). For reasonable parameters there is a sizeable range of r values in which these conditions hold. $S^{clr} - R^{clr}$ is maximum at $x = 1$, which leads to the precipitation maximum there; at the same time S, and thus in steady state also E is minimized there by the cloud-radiative feedbacks. These same feedbacks flatten the SST.

Obtaining the coexistent evaporation minimum and precipitation maximum in the fixed-SST system with finite τ_c is possible, but difficult, because the negative feedbacks that constrain E and the SST in the coupled system are not present. The SST has to be prescribed to a profile very close to one obtained as a solution (with the desired coexistent E minimum and P maximum) from the

coupled model. In the absence of the coupled feedbacks, slight deviations will eliminate either the E minimum or the P maximum.

The physical argument this leads to is that both the evaporation minimum and precipitation maximum result from the combination of

- the maximum in the clear-sky surface forcing in the warm pool, which results from there being a longitudinal minimum in the divergence of ocean heat transport and an equatorial maximum of annally-averaged clear-sky insolation;
- cloud-radiative feedbacks;
- the surface energy budget (i.e., thermal ocean coupling).

The surface wind speed is viewed as irrelevant because it can be viewed as determining E only for fixed SST. Once the surface energy budget must balance, we have $S = E$ in steady state, so E is constrained independently of the wind speed. If we change the wind speed, the surface humidity difference $q_s^* - q_s$ must change, which can change either or both of q_s or q_s^*, the latter implying an SST change.

While this argument is an improvement on any based on a fixed SST, there are still (at least) two weaknesses in it. One is that there may be spatial variations in M, which if large enough could allow P to differ in qualitative structure from $E - R$. We do not address this further here, but note that the latest estimates do not suggest large variations in M (Yu et al., 1998).

The more serious problem is our neglect of potential atmospheric feedbacks on ocean dynamics. In our model, ocean dynamics are encapsulated by specifying $S(x)$, which can include a contribution due to ocean heat flux divergence. $S(x)$ is treated as an external control which does not interact with the predicted atmospheric circulation. (Seager et al., 1988; Gent, 1991). Seager et al. (2003) have shown that this may be an inappropriate assumption for understanding the existence of the evaporation minimum in the equatorial warm pool. They used an ocean GCM coupled to an atmospheric mixed layer model to focus on the evaporation minimum in particular (as opposed to the precipitation maximum, since their model does not simulate precipitation). They found that while the shortwave cloud feedback did make a contribution toward inducing the evaporation minimum, a larger role was played by feedbacks between evaporation and ocean heat transport. Although the divergence of the latter is a small contributor to the heat budget of the present warm pool, nonetheless in the results of Seager et al. it is found to exert a strong control on the solution in the sense that if other conditions were to change, the ocean heat transport divergence could change significantly, resulting in feedbacks which would tend to maintain the evaporation minimum. This example shows both the value and the limitations of simple models including only a restricted set of processes. On the one hand, such models can aid in the development of simple, unambiguous hypotheses for the chains of cause and effect leading to certain observed features. On the other hand, the excluded processes may turn out to be important.

v. Stability and time-dependence For the fixed-SST, SQE model, as mentioned above $M_{eff} = 0$ delineates the critical value of r at which the steady solution is marginally stable. Once τ_c becomes finite, whether the system is coupled or not,the stability criterion is modified and stable solutions can persist for slightly negative M_{eff}. However, qualitatively the situation is the same. For sufficiently large r, the solution becomes unstable to time-dependent disturbances. For the fixed-SST case, numerical integrations show that these time-dependent disturbances are not well behaved, but that the precipitation blows up in amplitude as the precipitating region shrinks to the grid scale. For the coupled case, well-behaved oscillations develop, first at $x = 1$, and then for larger r, increasing their domain of influence until soon the entire precipitating region exhibits time-dependent behavior. These oscillatory solutions were mentioned but not explicitly presented by Sobel (2003). Here we show a Hovmoeller plot of the precipitation field from such a solution, in fig. 4. The model configuration used to obtain this simulation is similar to that used by Sobel, but different enough that some explanation is required.

The solution shown in Fig. 3, and all those shown in Sobel (2003), were computed using a mixed layer depth of $1m$. This was done to achieve fast integration to steady state. This parameter choice was not discussed by Sobel, since he focused only on steady-state solutions for which the mixed layer depth drops out of the equations. However, we now understand that the mixed layer depth can be important in determining the stability of the steady solution. Unfortunately, we did not appreciate this at the time, and did not carefully explore sensitivity to mixed layer depth. It turns out that the

solutions shown by Sobel (2003) become unstable to time-dependent perturbations for mixed layer depths only slightly larger than $1m$, while observed mixed layer depths for warm tropical oceans tend to be in the range 10-50m. Thus for other parameters kept fixed, some of Sobel's steady solutions (e.g. at $r = 0.2$) are not stable for realistic mixed layer depths. On the other hand, Sobel used a rather small value for the convective time scale, $\tau_c = 0.2d$, which tends to make the system quite a bit more unstable than it would be for a larger, more appropriate value, on the order of 1 d. So, replacing Sobel's parameter choices with more realistic ones for both mixed layer depth and τ_c, the effects of these two parameter changes will tend to cancel and one may expect to obtain steady solutions for approximately the same range of r as shown by Sobel, if the other parameters are also kept the same. This turns out to be true *if* the formulation (7) is used for the dry static stability, but *not* if (6) is used, for essentially the reasons discussed in section iii. . The solution shown in fig. 4 thus uses a model and parameter values identical to those used by Sobel (2003) to produce fig. 3, except:

- $\tau_c = 0.7$ d and the mixed layer depth is 20 m, to increase realism as discussed above
- r is raised to 0.25 to render the steady solution unstable and generate time-dependent behavior, and
- (7) is used.

[Figure 4 about here.]

The figure shows eastward-propagating oscillations in rainfall in the eastern part of the domain. The period is on the order of $40d$. We view the propagation dynamics of these disturbances as unworthy of study, since the system as formulated contains none of the standard equatorial wave modes (Kelvin, Rossby etc.), which if present would presumably modify the propagation dynamics qualitatively as well as quantitatively. The fact that the propagation is eastward is not deemed to be significant, and in fact disturbances sometimes propagate westward for other parameter values, particularly right near $x = 1$. The phase speed of the disturbances is particularly irrelevant since its dimensional value scales linearly with the domain size, for the same reason that u does — namely, that the domain size drops out of the dynamical equations of this model due to WTG!

What is of most interest is the dynamics of the instability which generates the disturbances and selects the time scale. Since horizontal advection has only a weak effect on the disturbances due to the weak moisture gradient in the convective region, it seems reasonable to simplify the problem still further, to a single horizontal location, in order to study them.

c. Single-column, time-dependent model

Sobel and Gildor (2004) studied the equations from the preceding section with horizontal moisture advection omitted, in which case the dynamics of a single horizontal location can be treated independently of others and we have a zero-dimensional coupled model:

$$M_S \delta = P - R, \tag{25}$$

$$\hat{b}\frac{\partial q}{\partial t} - M_q\delta = E - P, \tag{26}$$

$$\frac{\partial T_S}{\partial t} = S - E. \tag{27}$$

Sobel and Gildor viewed this as a model for variations of SST on an intraseasonal time scale, in an idealized context where the horizontal propagation associated with the Madden-Julian Oscillation (MJO) is ignored, though the latter can be addressed in a crude way. The best observational context for thinking about intraseasonal SST variability without directly considering the MJO is provided by Waliser (1996), who looked at the dynamics of "hot spots", or locations where the SST becomes greater than 29.5 C for at least a month. The occurrence of hot spots tends to be preceded by clear skies, high surface insolation, and low surface wind speed and the small surface fluxes. Once the hot spot develops, however, it tends to destabilize the atmosphere to deep convection, which eventually occurs, and the associated cloudiness and surface winds eventually cool the ocean surface, shutting the hot spot down. At that point, the atmosphere over the cooled sea surface will become more stable to deep convection, and we expect convection to stop. This will lead to clear skies, thus warming SST, and we can imagine an oscillatory cycle which continues like this. The MJO will modify the picture by producing a somewhat independent forcing mechanism to drive the variations, but we expect that understanding the dynamics without an MJO will help us to understand how the MJO couples to the same convective-radiative-ocean mixed layer dynamics.

In this model, the parameter r in (15) may be viewed as representing not only shortwave cloud-radiative feedbacks associated with precipitation, but also the feedback of increased surface fluxes

associated with the development of 'cold pools' and convectively enhanced gustiness where there is more precipitation. Under the assumption that the total cloud-radiative feedback vanishes at TOA, it acts just like a surface flux, simply moving energy between ocean and atmosphere. Additionally, variations in surface turbulent fluxes (mainly evaporation) and radiative fluxes are found to be nearly in phase on intraseasonal time scales. Because of these two facts, both feedbacks can be empirically modeled by the single parameterization (15).

i. Linear results

[Figure 5 about here.]

Fig. 5 shows growth rate and frequency as a function of parameters for the system obtained by linearizing (25)-(27). The linear equations, and their closed-form solutions from which these plots were generated, can be found in Sobel and Gildor (2004). Sensitivity is shown to the two most important parameters, r and τ_c, and also to the mixed layer depth. The blacked-out regions are those in which the linear frequency is zero, that is, the linear calculation predicts pure, non-oscillatory growth or decay. The growth rate is positive only for large r and small τ_c. There is only a fairly narrow region around the marginal stability curve, in $r - \tau_c$ space, in which the linear frequency is nonzero. In that range, the frequency is intraseasonal to subannual (0.1 corresponds to $10 \times 2\pi$ or around 60 days). In the SQE limit $\tau_c \to 0$, the range of r supporting oscillations shrinks to zero width, and the marginal stability criterion for growing (but now non-oscillatory) solutions

reduces to $M_{eff} = 0$. This again emphasizes that while SQE is a useful guide to the finite-τ_c behavior when $M_{eff} > 0$ and steady-state solutions are obtained, it is not so useful when M_{eff} becomes negative.

ii. Nonlinear results

[Figure 6 about here.]

Fig. 6 shows a nonlinear simulation in the regime in which the system is linearly unstable. The precipitation P, evaporation E, radiative cooling R, surface shortwave flux S, SST, and surface humidity q_s, are shown as functions of time. Note that the evaporation is that computed directly from (13); it does not explicitly include the "extra" evaporation variations which we might take to be included with the cloud-radiative feedback.

We see vaguely square-wave type variations in precipitation, R and S. Detailed features, such as the particular shape of the precipitation pulses and their duration relative to the duration of non-precipitating periods, are dependent on parameters. The SST has more sawtooth-like variations. The oscillation overall has characteristics of a recharge-discharge oscillation. The "discharge" is the flux of moist static energy from ocean to atmosphere (by radiative processes as well as surface fluxes), and horizontal export of that moist static energy in the atmosphere associated with the precipitating phase, and the "recharge" is the buildup of energy in the ocean associated with the suppressed phase, when the atmosphere is descending and the SST is increasing[4]. An interesting

[4]The analogy to a discharging capacitor should not be taken too literally, because the energy budget of the present

prediction of this model is that the growth rate for the instability increases with mixed layer depth. This is contrary to what we might expect, since with larger mixed layer depth, the SST can vary less and we might expect this to lead to less overall variability, but viewing the variability as a recharge-discharge oscillation helps us to understand this, since the mixed layer is the capacitor for the system; without storage capacity there can be no recharge-discharge.

Watterson (2002) indeed found, in an AGCM coupled to a constant-depth ocean mixed layer, that intraseasonal variability tended to decrease with mixed layer depth. This contradicts the results above, if we view the growth rate as a proxy for the variance we expect in a nonlinear simulation. To explain this, Sobel and Gildor (2004) forced the linear model, in a weakly stable regime, with an imposed atmospheric oscillation in the heating ($P - R$), of intraseasonal frequency, to represent an atmospheric MJO which would exist in the absence of coupling. The model response showed a peak amplitude near 10-20m (the value of mixed layer depth which leads to a linear frequency near the forcing value) with decay at larger depths, as found by Watterson, but also decay at smaller depths, not investigated by Watterson. More recent simulations performed by Eric Maloney (pers. comm.), with the NCAR CCM3 coupled to a constant-depth ocean mixed layer, bear out the simple model prediction. These simulations, which are ongoing and will be reported in more detail in due course, show a dramatic decrease in the magnitude of precipitation variability as mixed layer depth is reduced below about 10 meters.

model is not closed; moist static energy is generally being either exported or imported from the column.

4. Conclusions

We have described a set of simple models for aspects of the tropical climate. These models represent the divergent tropical circulation as a product of feedbacks between SST, surface fluxes, deep convection, and radiation, with the humidity field being the primary prognostic atmospheric variable modulating these feedbacks. The basic model ingredients are the Neelin-Zeng QTCM equations, the weak temperature gradient approximation, the neglect of rotation and the assumption of slab-symmetry in latitude so that only the along-equatorial circulation is modeled. The strict quasi-equilibrium (SQE) approximation may also be used, either in the models themselves or in analytical work aimed at understanding the results when the convective time scale, τ_c, is finite. SQE is a good approximation in the sense that many features of the steady solutions are insensitive to increases in the convective time scale from zero up to at least realistic values on the order of $\sim 1\ d$. The stability of the steady solutions to time dependent perturbations, on the other hand, is quite sensitive to variations in τ_c in this range, so that SQE may under some circumstances be quite inaccurate for understanding the stability and possible time-dependent behavior of finite τ_c solutions.

When SST is fixed, the cloud-radiative feedback is a net source of energy to the system, and strongly shrinks the convective region in steady state. For strong enough feedback, the convective region shrinks to a single point and no steady solution can be found. In fact, the system becomes badly behaved, and numerical simulations suggest that even time-dependent simulations blow up after a finite time.

When coupling to an ocean mixed layer is added, the cloud-radiative feedback has no effect on the size of the convective region, the latter being controlled by the clear-sky surface energy budget. The model in this configuration is able to robustly produce a coexistent evaporation minimum and precipitation maximum, as are observed, but perhaps for reasons which are only partly correct. More recent work suggests that feedbacks between ocean heat transport and the atmospheric circulation, which are neglected in our model, plays a large role in creating this feature.

When the cloud-radiative feedback parameter is increased past a threshold value, the coupled model becomes unstable to free oscillations of intraseasonal to subannual period. The strength of the instability is most sensitive to the cloud-radiative feedback parameter (which can also be thought of as representing the surface flux feedback) and the convective time scale. The onset of instability is well captured by a linear analysis, but the oscillations in the full system tend to be nonlinear, with a recharge-discharge character and periods of zero precipitation alternating with rainy periods. Although the growth rate of the instabilities increases (slowly) with mixed layer depth, in a forced calculation in a weakly stable parameter regime the amplitude of the response has a peak near 10-20m, decreasing for both larger and smaller mixed layer depths. The decrease at larger depths was found in an AGCM coupled to a mixed layer ocean by Watterson, while the decrease at smaller depth appears to also occur and is being investigated in ongoing work.

Acknowledgments

We thank Isaac Held, David Neelin and Richard Seager for discussions. AHS acknowledges support from NSF grant DMS-01-39830 and a fellowship from the David and Lucile Packard foundation. CB and MP acknowledge support from NSF grant DMS-0139794. Any opinions, findings, conclusions or recommendations expressed in this paper are those of the authors and do not necessarily reflect the views of the sponsors.

References

Betts, A. K., 1986: A new convective adjustment scheme .1. observational and theoretical basis. *Q. J. R. Meteorol. Soc.*, **112**, 677–691.

Bretherton, C. S., M. E. Peters, and L. Back, 2004: Relationships between water vapor path and precipitation over the tropical oceans. *J. Climate*, **submitted**.

Bretherton, C. S. and A. H. Sobel, 2002: A simple model of a convectively-coupled Walker circulation using the weak temperature gradient approximation. *J. Climate*, **15**, 2907–2920.

Emanuel, K. A., J. D. Neelin, and C. S. Bretherton, 1994: On large-scale circulations in convecting atmospheres. *Q. J. R. Meteorol. Soc.*, **120**, 1111–1143.

Gent, P. R., 1991: The heat budget of the TOGA COARE domain in an ocean model. *J. Geophys. Res.*, **96**, 3323–3330.

Harrison, E. F., P. Minnis, B. R. Barkstrom, V. Ramanathan, R. D. Cess, and G. G. Gibson, 1990: Seasonal-variation of cloud radiative forcing derived from the earth radiation budget experiment. *J. Geophys. Res.*, **95**, 18687–18703.

Hartmann, D. L., L. A. Moy, and Q. Fu, 2001: Tropical convection and the energy balance at the top of the atmosphere. *J. Climate*, **14**, 4495–4511.

Kiehl, J., 1994: On the observed near cancellation between longwave and shortwave cloud forcing in tropical regions. *J. Climate*, **7**, 559–565.

Neelin, J., 1997: *The physics and parameterization of moist atmospheric convection*, Kluwer Academic Publisher, chapter Implications of convective quasi-equilibrium for the large-scale flow. 413–446.

Neelin, J. D. and I. M. Held, 1987: Modeling tropical convergence based on the moist static energy budget. *Mon. Weath. Rev.*, **115**, 3–12.

Neelin, J. D. and N. Zeng, 2000: A quasi-equilibrium tropical circulation model: Formulation. *J. Atmos. Sci.*, **57**, 1741–1766.

Peters, M. E. and C. S. Bretherton, 2004: An idealized walker circulation coupled to an ocean mixed layer. *J. Climate*, **in preparation**.

Ramanathan, V., R. D. Cess, E. F. Harrison, P. Minnis, B. R. Barkstrom, E. Ahmad, and D. Hart-

mann, 1989: Cloud-radiative forcing and climate: results from the earth radiation budget experiment. *Science*, **243**, 57–63.

Seager, R., R. Murtugudde, A. Clement, and C. Herweijer, 2003: Why is there an evaporation minimum at the equator? *J. Climate*, **in press**.

Seager, R., S. E. Zebiak, and M. A. Cane, 1988: A model of the tropical Pacific sea-surface temperature climatology. *J. Geophys. Res.*, **93**, 1265–1280.

Shaevitz, D. A. and A. H. Sobel, 2004: Implementing the weak temperature gradient approximation with full vertical structure. *Mon. Weath. Rev.*, **submitted**.

Sobel, A. H., 2003: On the coexistence of an evaporation minimum and precipitation maximum over the warm pool. *J. Climate*, **16**, 1003–1009.

Sobel, A. H. and C. S. Bretherton, 2000: Modeling tropical precipitation in a single column. *J. Climate*, **13**, 4378–4392.

Sobel, A. H. and H. Gildor, 2004: A simple time-dependent model of sst hot spots. *J. Climate*, **in press**.

Sobel, A. H., J. Nilsson, and L. M. Polvani, 2001: The weak temperature gradient approximation and balanced tropical moisture waves. *J. Atmos. Sci.*, **58**, 3650–3665.

Su, H. and J. D. Neelin, 2002: Teleconnection mechanisms for tropical Pacific descent anomalies during El Nino. *J. Atmos. Sci.*, **59**, 2694–2712.

Waliser, D. E., 1996: Formation and limiting mechanisms for very high sea surface temperature: Linking the dynamics and the thermodynamics. *J. Climate*, **9**, 161–188.

Watterson, I. G., 2002: The sensitivity of subannual and intraseasonal tropical variability to model ocean mixed layer depth. *J. Geophys. Res.*, **107**, 10.1029/2001JD000671.

Yu, J.-Y., J. D. Neelin, and C. Chou, 1998: Estimating the gross moist stability of the tropical atmosphere. *J. Atmos. Sci.*, **55**, 1354–1372.

Zeng, N., J. D. Neelin, and C. Chou, 2000: A quasi-equilibrium tropical circulation model: Implementation and simulation. *J. Atmos. Sci.*, **57**, 1767–1796.

List of Figures

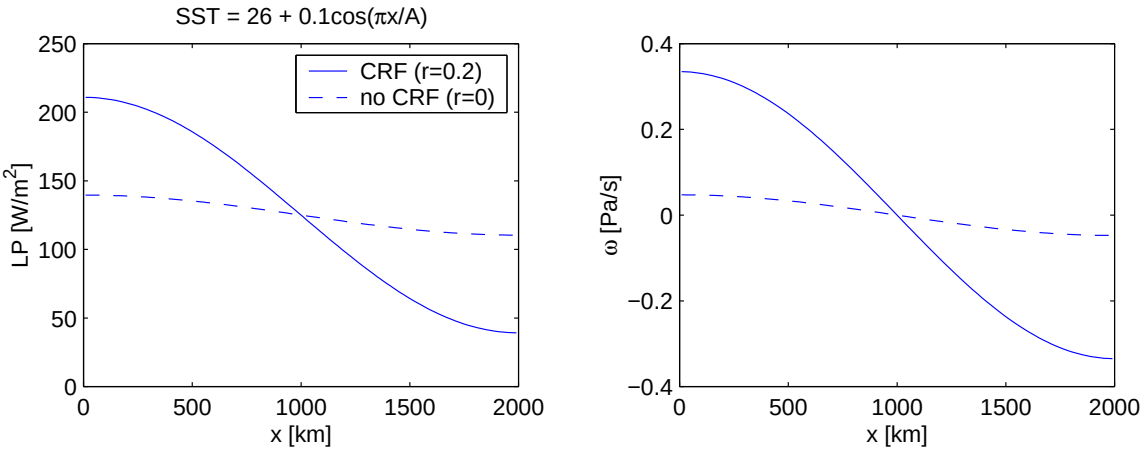

Figure 1: Modeled $\omega(x)$ (right) and precipitation (left) for ΔSST = 0.1 K. Convection extends throughout the domain. Actual vertical p-velocity is obtained by multiplying ω by the vertical structure function $\Omega(p)$ of which varies from 0 at the surface and tropopause to an extremum of -0.09 at 500 mb. The solid and dashed curves show steady-state solutions including and excluding cloud-radiative feedback (CRF), respectively. Figure taken from Bretherton and Sobel (2002).

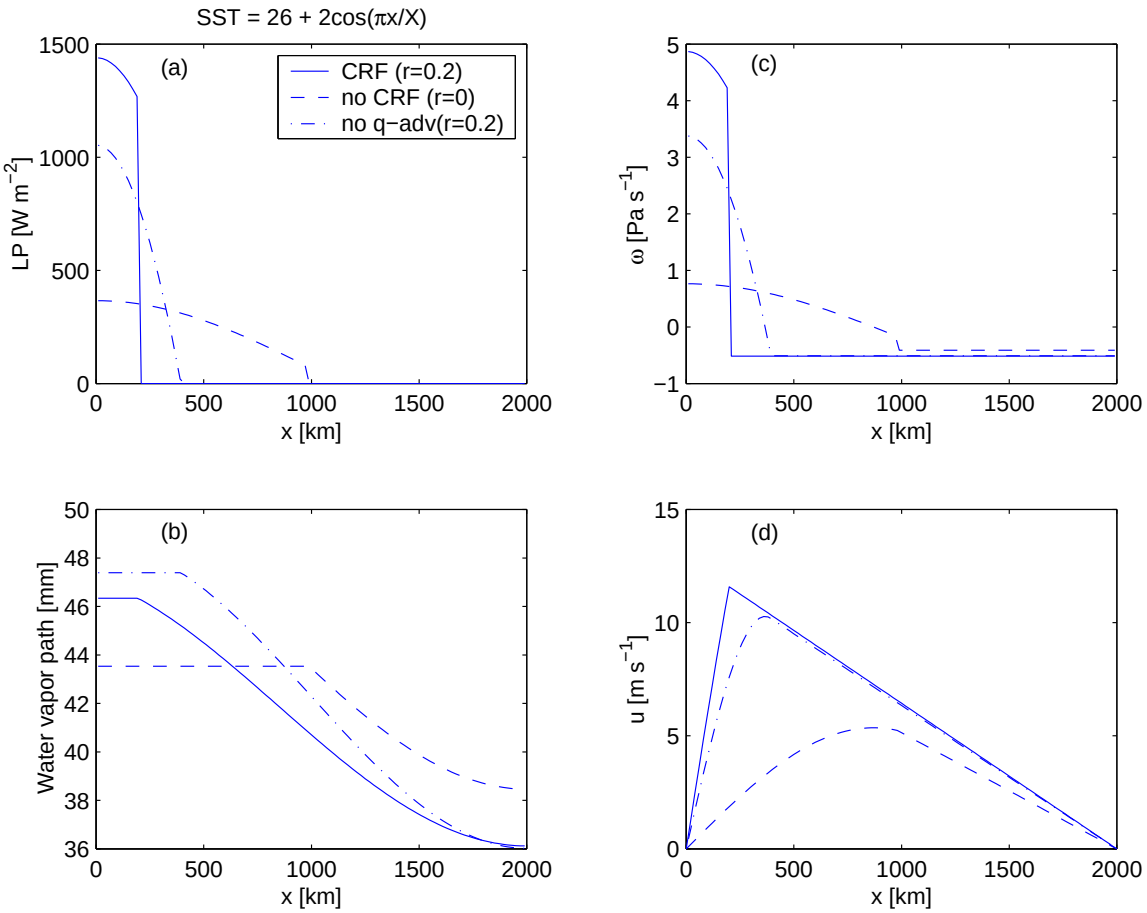

Figure 2: (a) Precipitation, (b) water vapor path, (c) vertical and (d) horizontal motion, for ΔSST = 2 K. In the latter two panels, the full two-dimensional fields are obtained by multiplying by the vertical structure functions. Solutions are shown with and without cloud-radiative forcing (CRF), and a solution with CRF but without horizontal moisture advection is also shown. Figure taken from Bretherton and Sobel (2002).

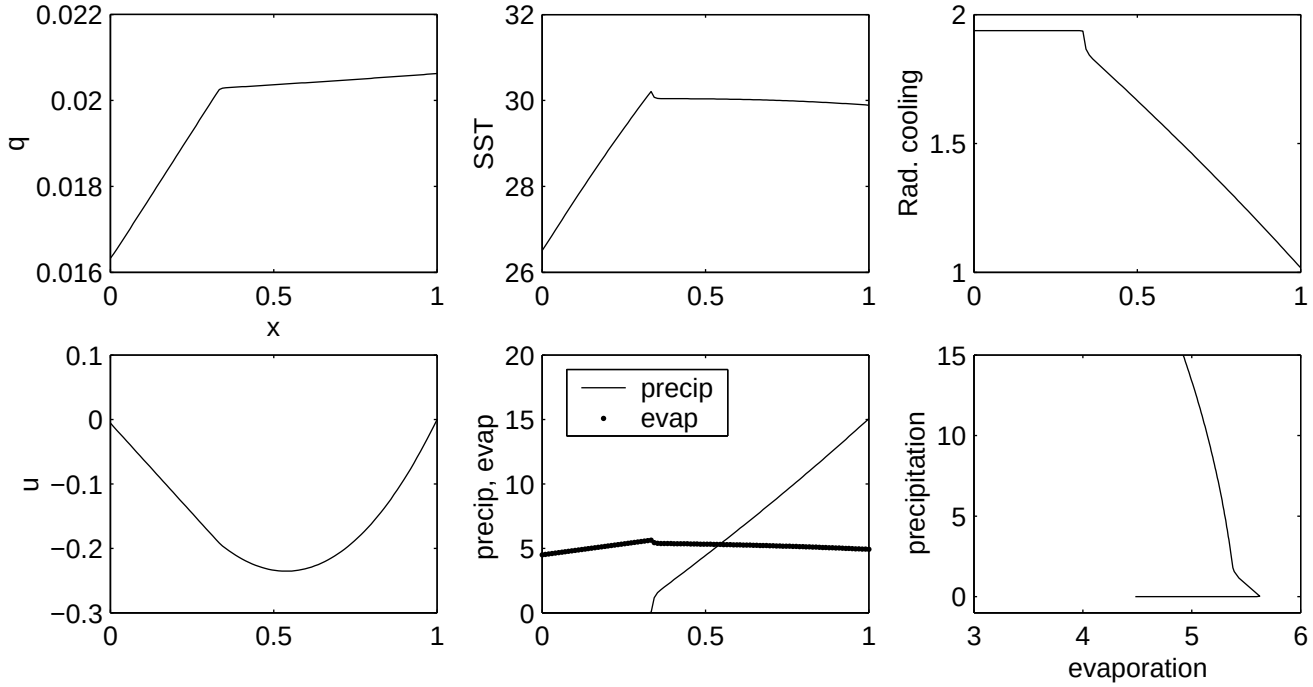

Figure 3: Steady solutions of the model coupled to an ocean mixed layer, with the cloud-radiative feedback parameter $r = 0.2$ and convective time scale $\tau_c = 1\ d$; see text for further details. From left to right and top to bottom, the first five panels show surface specific humidity ($kg\ kg^{-1}$), SST (°C), radiative cooling rate (°K d^{-1}), wind velocity (arbitrary units), and precipitation and evaporation ($mm\ d^{-1}$), vs. the horizontal coordinate x, while the last (bottom right) panel shows precipitation on the y axis and evaporation on the x axis. Figure taken from Sobel (2003).

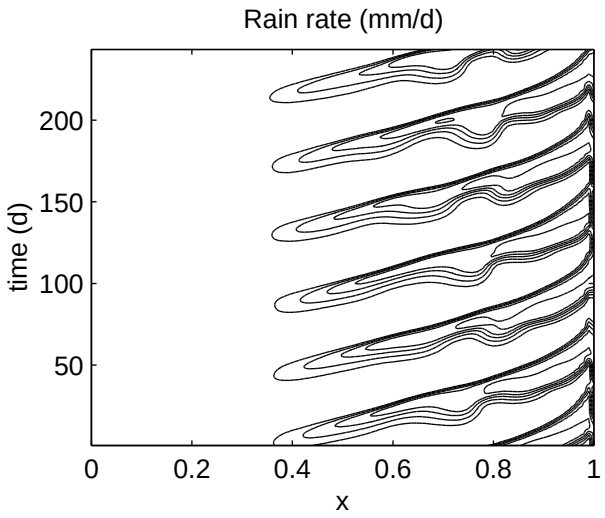

Figure 4: The precipitation rate ($mm\ d^{-1}$; contour interval $5\ mm\ d^{-1}$), as a function of longitude (x) and time, for a time-dependent solution of the 1D model coupled to an ocean mixed layer. The model and parameters are as in Sobel (2003), except that the mixed layer depth is $20m$, convective time scale $\tau_c = 0.7\ d$, and cloud-radiative feedback parameter $r = 0.25$, and the formulation (7) rather than (6) is used to compute the dry static stability.

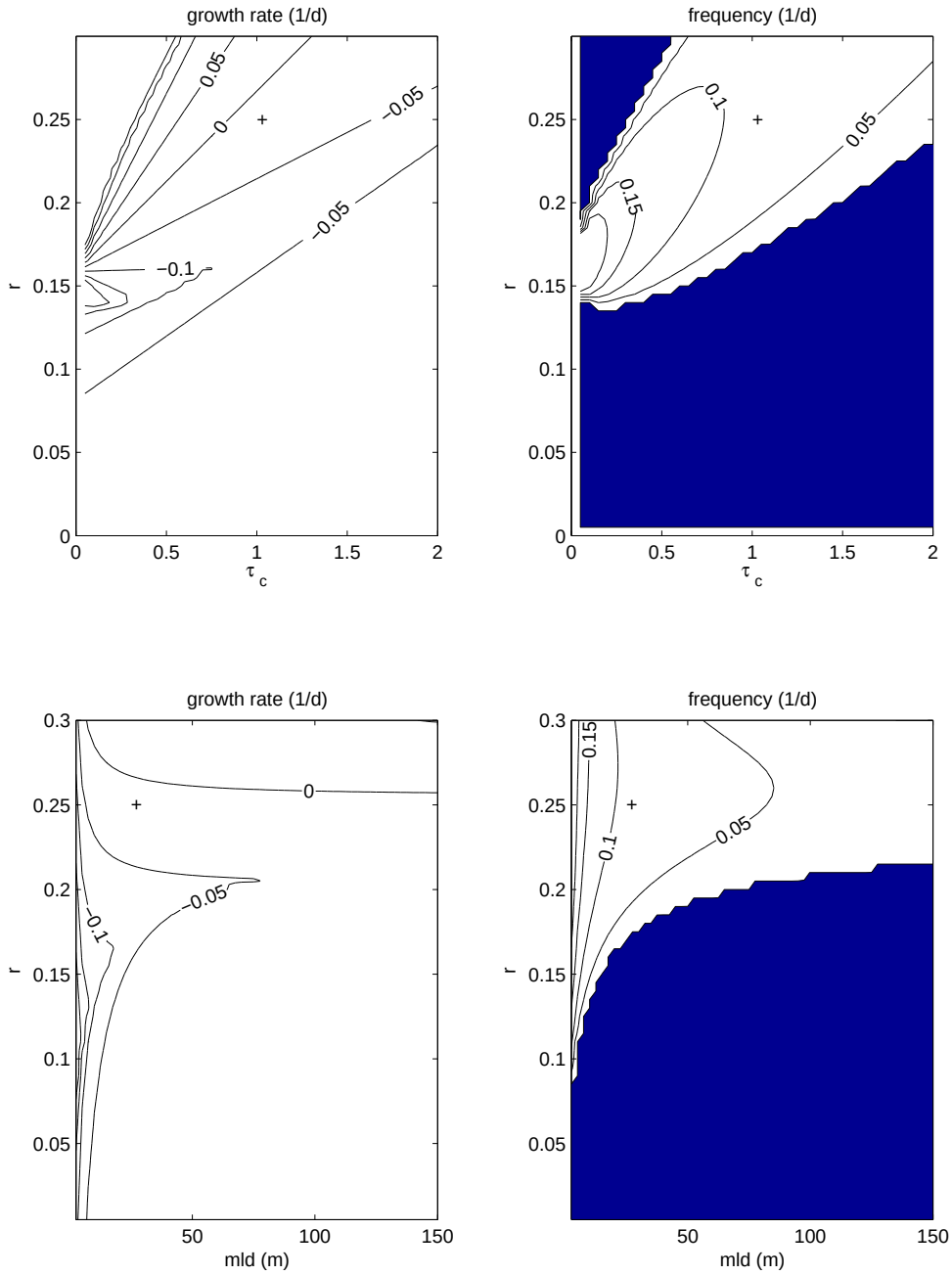

Figure 5: Linear growth rate and frequency as functions of cloud-radiative feedback parameter r and convective time scale (top) and mixed-layer depth (bottom). In the frequency plots, regions where the frequency is zero are filled. Plus symbols indicate the default parameter values given in table 1 of Sobel and Gildor (2003).

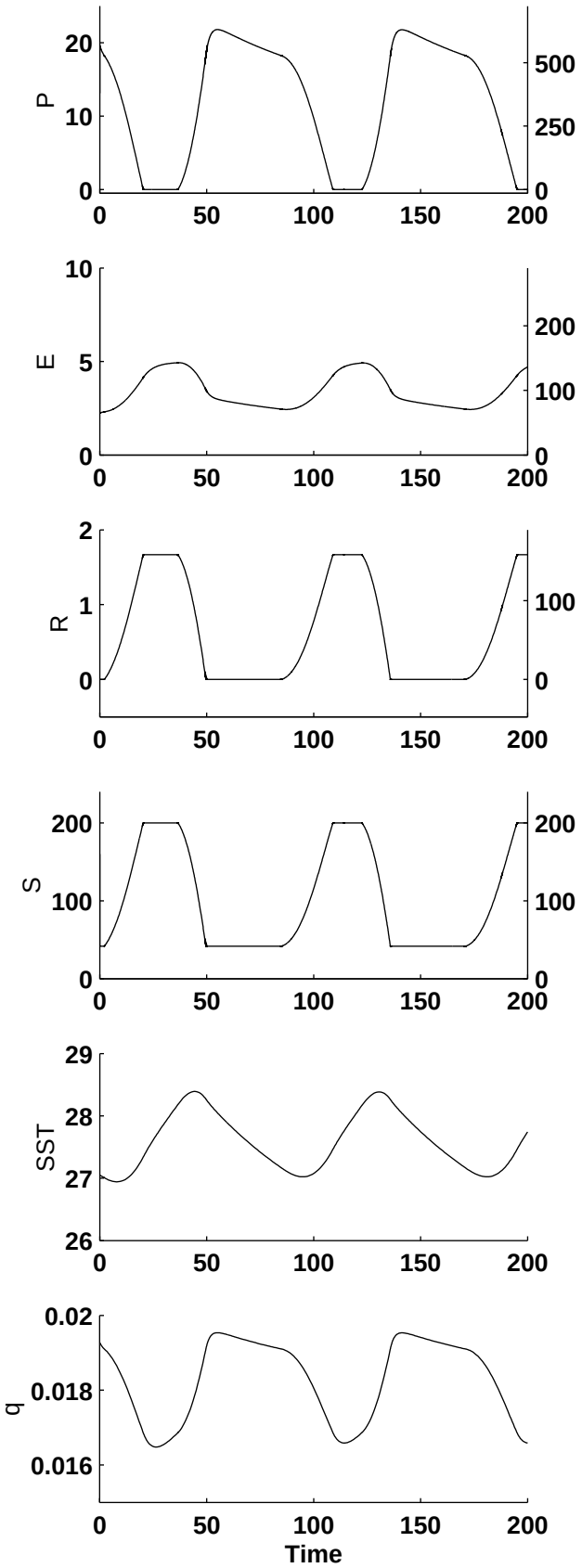

Figure 6: A nonlinear solution to the Sobel-Gildor model with $r = 0.3$ and $\tau_c = 1\ d$. From top to bottom: Precipitation (left axis $mm\ d^{-1}$, right axis $W\ m^{-2}$), evaporation (left axis $mm\ d^{-1}$, right axis $W\ m^{-2}$), Radiative cooling (left axis $K\ d^{-1}$, right axis $W\ m^{-2}$), net flux of short wave and long wave at the ocean surface (both axes ($W\ m^{-2}$), sea surface temperature ($^{\circ}$C) and specific humidity ($kg\ kg^{-1}$). Taken from Sobel and Gildor (2004).